Correlation between the magnetorefractive effect, giant magnetoresistance, and optical properties of Co-Ag granular magnetic films

V. G. Kravets, D. Bozec, J. A. D. Matthew, and S. M. Thompson
Department of Physics, University of York, Heslington, York YO10 5DD, United Kingdom

H. Menard and A. B. Horn
Department of Chemistry, University of York, Heslington, York YO10 5DD, United Kingdom

A. F. Kravets
Institute of Magnetism, 36 Vernadsky Street, 252142 Kiev, Ukraine
(Received 26 July 2001; published 9 January 2002)

Giant magnetoresistance (GMR), optical properties, and the infrared magnetorefractive effect (MRE) are studied in reflection for granular films of composition Co_xAg_{1-x} with x ranging from 0.1 to 0.7. From ellipsometry measurements it is shown that it is necessary to take into account finite-size effects in order to successfully model the optical data demonstrating the importance of the microstructure to the MRE. The ellipsometry data enable the variation in optical properties with Co concentration to be determined and incorporated into a model of the MRE. The MRE itself is calculated with a frequency- and spin-dependent conductivity. Both the experimental and theoretical analyses reveal a correlation between GMR and the MRE demonstrating the feasibility of using the MRE as a contactless method for measuring the GMR and for extracting fundamental spin-dependent scattering parameters.

DOI: 10.1103/PhysRevB.65.054415 PACS number(s): 72.15.Eb, 72.15.Lh, 78.30.Er

I. INTRODUCTION

In the last decade, there has been considerable interest in the experimental exploitation and theoretical interpretation of giant magnetoresistance (GMR).[1] GMR arises from spin-dependent scattering[2,3] and has been observed in magnetic multilayers (with alternating layers of magnetic and nonmagnetic materials) and in granular films (with magnetic clusters embedded in a nonmagnetic matrix).[4,5] More recently, the magnetorefractive effect (MRE) was proposed theoretically and proved experimentally by Jacquet and Valet.[6] The MRE exploits infrared spectroscopy to probe the change of reflection and transmission in the infrared region due to the change of conductivity when a magnetic field is applied to a system that exhibits GMR. Since its discovery, the MRE has been measured in transmission and reflection in a limited range of systems including both multilayers and granular films.[6–8] Correlation of the MRE with GMR has been experimentally demonstrated, proving the potential of the MRE as a contactless technique for the measurement of GMR.[9,10] The MRE differs from GMR in that it originates from both the optical and the transport properties of the thin film and attempts to model it are still in their infancy.[6–10] The dependence of the MRE on electrical conductivity offers the potential for the extraction of the fundamental material- and spin-dependent scattering parameters from measurements of the MRE.

In this paper we show that the correlation between the GMR and MRE depends on the wavelength regime. Material parameters such as grain size may affect the optical parameters differently than the electrical parameters. These parameters become significant at lower wavelengths and therefore in order to model the full spectrum, it is necessary to determine optical properties such as the dielectric function, the plasma frequency, and the optical relaxation.

The materials studied in this paper are giant magnetoresistive granular Co-Ag films. Such systems have been widely studied because of their large room-temperature magnetoresistance effect which has been seen to occur in a wide variety of granular nanostructures.[11,12] Co and Ag are imiscible since the surface free energy[13] of Co (2.71 J/m^2) is more than twice that of Ag (1.30 J/m^2) causing the Co to form clusters. There is also a very poor lattice match since fcc Ag has a lattice parameter that is 15% larger than that of fcc Co. The optical and magneto-optical properties of Co-Ag granular films in the visible spectral region are strongly dependent on the relative composition of Co and Ag and on structural material parameters such as grain size that will vary with deposition parameters.[14,15] The MRE has previously been observed in Co-Ag granular films and it has been demonstrated that the self-averaging effect can be applied to such materials.[9,10]

In this paper, optical properties, GMR, and the MRE reflection effects in Co_xAg_{1-x} magnetic granular films have been studied at room temperature over a wide range of Co concentrations. The optical measurements were made using spectroscopic ellipsometry,[16–18] which has been proved to be a powerful optical tool for the nondestructive study of electronic structure. The technique measures the dielectric response functions, which contain information on the optical transitions between the occupied and unoccupied electronic band states.[19] The optical properties were modeled using the Drude model,[17,18] which was modified to include spin-dependent scattering rates calculated using the model for GMR granular systems by Zhang and Levy.[2,12] A value for the relative dielectric constant for Ag-rich samples was determined from the ellipsometry results in the visible spectral region and then this value was used in the subsequent calculation of the MRE. The MRE was calculated with a model

containing the frequency- and spin-dependent conductivity that influences the complex refractive index of the thin film.[8,20]

II. SAMPLE PREPARATION AND EXPERIMENTAL DETAILS

Granular films of Co-Ag were prepared by coevaporation of Co and Ag using two independent electron-beam sources at room temperature on sapphire substrates. The base pressure during deposition was less than 10^{-4} Pa. Cobalt atomic concentrations varied from 0% to 90%. The deposition rate varied from 0.1 to 0.2 nm/s and the total thickness of the deposited films was approximately 200 nm. The composition of the films was confirmed using energy dispersive x-ray spectroscopy and Auger electron spectroscopy.

The structure of the films was studied by x-ray diffraction with Cu $K\alpha$ radiation. As-deposited Co_xAg_{1-x} (x at. %) magnetic granular films exhibit single-phase fcc peaks at $2\theta \approx 38°$ from the Ag (111) planes for all samples. With increasing Co content, x, the peak position shifts to a higher angle, and the intensity of a broad peak around $2\theta \approx 44°$ increases, which arises from both the fcc Ag (200) and fcc Co (111) planes.

The microstructure of the Co-Ag films was determined by high-resolution transmission-electron microscopy. With x increasing from 0.1 to 0.7 the average grain size increased from 1 to 5 nm. This is in agreement with values derived from superconducting quantum interference device magnetometry and nuclear-magnetic-resonance measurements.[21]

The optical properties of the samples were also studied by means of spectroscopic ellipsometry in the 1.0–4.2-eV photon energy region (0.3–1 μm) at a fixed angle of incidence of $\phi_0 = 72°$. Schematically, the spectroellipsometer is a polarizer-sample-analyzer system with the fixed polarizer azimuth equal to 45°. The analyzer is rotated in steps of 45° (by the Beattie method). Through measurement of the complex reflectance ratio ρ ($=r_p/r_s$) of the p (parallel) and s (perpendicular) field components of the light beam, defined with respect to the plane of incidence of the sample, the complex dielectric function ε^* can be obtained from the following equations using a semi-infinite medium model (air and sample).[16,18]

$$\sqrt{\varepsilon^*} = \sqrt{\varepsilon_1 + i\varepsilon_2} = n^* = n - ik = \sqrt{\sin^2\phi_0 + \sin^2\phi_0 \tan^2\phi_0 \frac{(1-\rho)^2}{(1+\rho)^2}} \qquad (1)$$

Ellipsometry measurements were performed at room temperature in air. The corresponding optical constants n and k, as well as the dielectric functions $\varepsilon_1 = n^2 - k^2$ and $\varepsilon_2 = 2nk$, were calculated (where ε_1 and ε_2 are the real and imaginary parts of the complex dielectric function ε^*, respectively). The error in the values of n and k depends on the sample size and surface quality, but lies in the region of 2%–3%. The optical conductivity is described by the relationship $\sigma(\hbar\omega) = \varepsilon_2\omega/4\pi$ (ω is the angular frequency of light and $\hbar$ is the Planck constant) at photon energy $\hbar\omega$. $\hbar\omega$ was varied by 0.1-eV steps within the spectral region investigated.

The magnetoresistance was measured by a dc method using a four-terminal configuration with a magnetic field up to 7 kOe at room temperature.

Infrared reflection measurements were made between 2 and 14 μm using a Mattson RS1000 Fourier-transform infrared reflection (FTIR) at 4-cm^{-1} resolution and a liquid-nitrogen-cooled HgCdTe photoconductive detector. The infrared beam was presented to and collected from the sample to study by two off-axis parabolic mirrors (focal length $f = 30$ cm) giving an angular spread of approximately $\pm 3°$ for the incident beam. The incidence angle for all measurements was set at 75° and magnetorefractive measurements were performed up to a maximum field of 4 kOe. The sample chamber was flushed with nitrogen gas to reduce the influence of water vapor and CO_2 on the reflection spectrum. Data obtained from the FTIR spectrometer were analyzed by taking three consecutive spectra: S_1 at zero field, S_2 in an applied field, and S_3 in zero field again. S_1 and S_3 were averaged out to take into account the change of background (e.g., drift of the detector response and buildup of water ice onto the detector). The MRE was then calculated as

$$\text{MRE}\ \ (\%) = \frac{0.5\times(S_1+S_3)-S_2}{S_2}\times 100, \qquad (2)$$

which corresponds to a relative change in reflectivity,

$$\Delta R/R\ \ (\%) = \frac{[R(H=0)-R(H_{\max})]}{R(H_{\max})}\times 100 \qquad (3)$$

with $H_{\max}$ equal to 4 kOe.

III. EXPERIMENTAL RESULTS

A. Ellipsometry measurements

The complex dielectric function $\varepsilon^*(\hbar\omega) = \varepsilon_1(\hbar\omega) + i\varepsilon_2(\hbar\omega)$ provides information about the interband transitions that are related to the combined density of states at high-symmetry points of the Fermi surface.[17,22] However, these transitions are also affected by structural properties such as grain size. The variation of the real part $\varepsilon_1(\hbar\omega)$ and the imaginary part $\varepsilon_2(\hbar\omega)$ of the dielectric function as a function of composition are shown in Figs. 1 and 3 for Co-rich compositions and Figs. 2 and 4 for Ag-rich compositions, respectively.

In contrast to the sharp threshold absorption edge typical for pure Ag films, a significant interband broadening is observed in these Co-Ag films due to the confinement of the electronic mean free path that results from the presence of grain boundaries.[23] The magnitude of the imaginary part of the dielectric function of these Co-Ag granular films is strongly enhanced in the energy region 1.5–3 eV (Figs. 3 and 4), especially for the Co-rich compositions shown in Fig. 3. The enhancement in this wavelength region is expected to reduce the values of $\varepsilon_2(\hbar\omega)$ in the infrared (IR) region. The real and imaginary parts of $\varepsilon(\hbar\omega)$ both show a systematic shift with increasing Ag content from Co-like optical con-

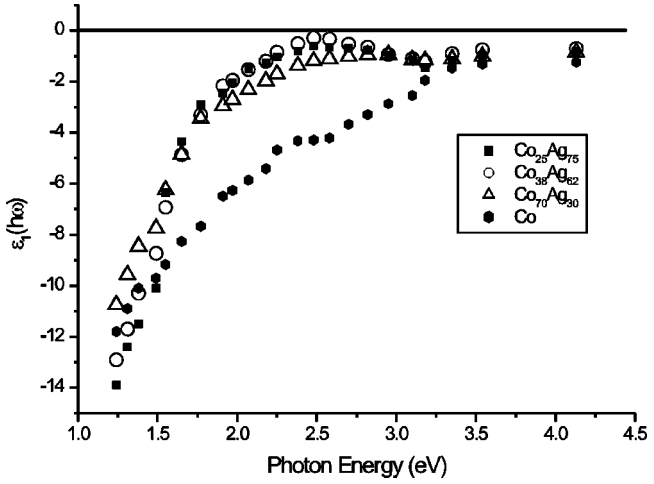

FIG. 1. The real part $\varepsilon_1(\hbar w)$ of the complex dielectric tensor as a function of the incident photon energy for different concentrations of Co.

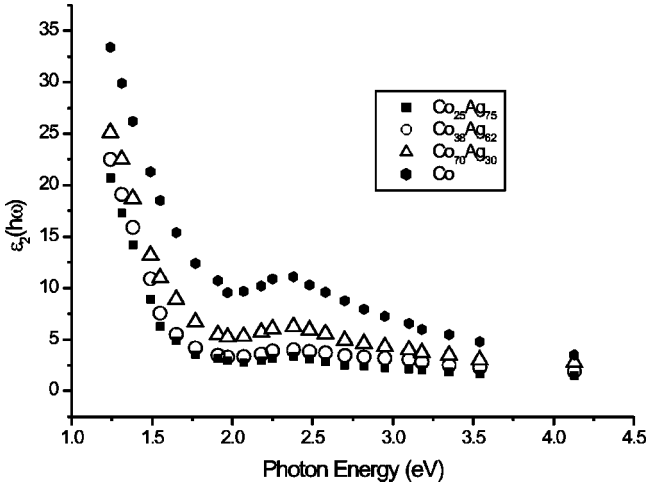

FIG. 3. The imaginary part $\varepsilon_2(\hbar w)$ of the complex dielectric tensor as a function of the incident photon energy for different concentrations of Co.

stants to Ag-like constants. With increasing Ag content the peak in the $\varepsilon_2(\hbar\omega)$ spectra around 2.4 eV decreases and the dip near 3.2 eV emerges (Figs. 3 and 4).

For metallic materials, plasma oscillation occurs at the spectral position ω_P, where $\varepsilon_1(\hbar\omega)\approx 0$, and $\varepsilon_2(\hbar\omega)$ is small.[17] These conditions are satisfied for Ag-rich Co_xAg_{1-x} granular films with $x=0.10$ and 0.12 shown in Figs. 4 and 2. For these films, a change of sign from negative to positive for the real part $\varepsilon_1(\hbar\omega)$ of the dielectric function at a photon energy of $\hbar\omega\approx 3.5$ eV can be observed, which, combined with the small value of $\varepsilon_2(\hbar\omega)$ in this region, leads to a plasma frequency of $\approx$3.4 eV. If Ag metal were a free-electron metal (i.e., if the response of the *d* electrons is neglected), it would have a plasma frequency of 9.1 eV but the plasma oscillations are modified by interband transitions involving *d* electrons so that the plasmon energy observed by electron energy-loss spectroscopy is 3.8 eV.[24] Here, the plasma frequency is further affected by the granular nature of the films.[19,14] This variation in the dielectric tensor between the samples due to both the composition and structure will affect the values of *n* and *k* and consequently the reflectivity from Eq. (1).

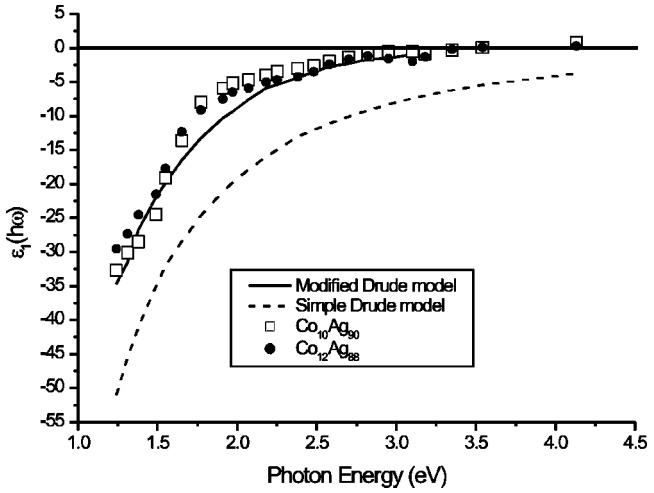

FIG. 2. The real part $\varepsilon_1(\hbar w)$ of the complex dielectric tensor as a function of the incident photon energy for Ag-rich granular films. The Drude model assumes $\varepsilon_r=1$ and uses the value of τ corresponding to that for pure Ag. The modified Drude model assumes $\varepsilon_r=3.5$ and a lower τ value to take into account the grain-size effects.

B. GMR and MRE measurements

Figure 5 shows the dependence of the magnetoresistance as a function of Co concentration. A maximum value of GMR of 15.3% for a field change of 7 kOe was obtained at a Co concentration of approximately 26%. The majority of the resistance change occurs for magnetic-field values below 4 kOe. Above 4 kOe, the resistivity of the films decreases slowly, but has not saturated for magnetic fields approaching 7 kOe.

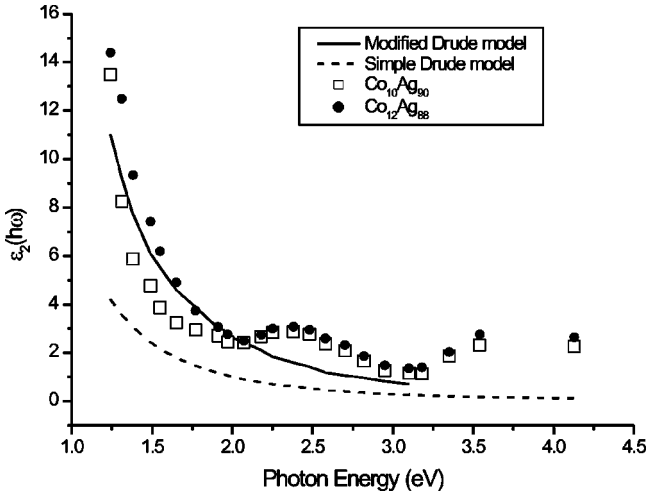

FIG. 4. The imaginary part $\varepsilon_2(\hbar w)$ of the complex dielectric tensor as a function of the incident photon energy for Ag-rich granular films.

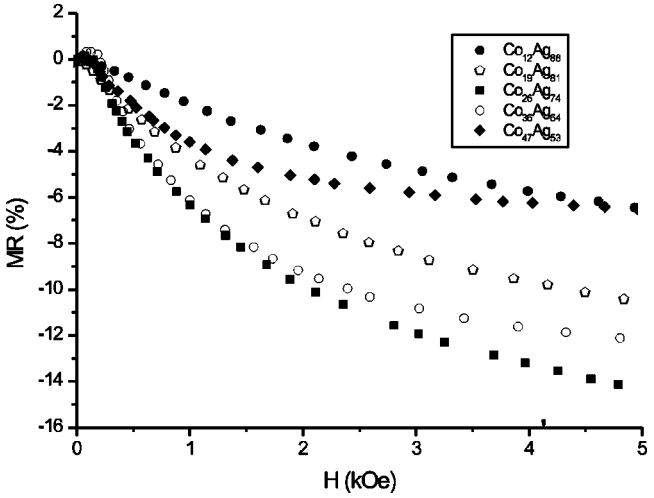

FIG. 5. Magnetoresistance as a function of Co concentration.

Figure 6 shows the relative change of infrared reflection for a single sample of $Co_{38}Ag_{62}$ as a function of wavelength for different values of the applied magnetic field. The MRE was calculated using Eq. (2). The change in reflection due to the applied field increases with increasing wavelength, with no saturation observed in the wavelength range (2–14 μm). The sharp peak observed at $\lambda \approx 4$ μm is due to the presence of a residual amount of CO_2 gas in the measuring chamber. The increase in noise above ≈ 14 μm is due to the limitations of the detector.

Figure 7 shows the MRE for a field difference of 4 kOe as a function of Co concentration from 12% to 47%. A maximum of the MRE of 0.75% for $\lambda = 14$ μm was observed for the sample containing 38% Co. As the concentration of Co is further increased to 47% of Co, the MRE decreases.

IV. INTERPRETATION

A. Optical properties

In general, the $\varepsilon(\hbar\omega)$ is related to the electronic properties of a material. If the solid film is a good conductor, like a noble metal (e.g., Ag), the optical wave interacts mainly with conduction electrons and, according to the Drude model,[17,18] the plasma frequency ω_P of the electron gas plays a very important role. The observed dielectric function of a 200-nm-thick Co film (Figs. 1 and 3) is like that observed in fcc Co films, where $\varepsilon_2(\hbar\omega)$ exhibits a peak near 2.4 eV, and $\varepsilon_1(\hbar\omega)$ shows a smooth variation with frequency. The physical origin of this phenomenon is related to the minority $3d$ bands of Co that cut the Fermi level giving rise to a complicated Fermi-surface crossing resulting in numerous interband transitions. The feature in the $\varepsilon_2(\hbar\omega)$ spectra around $\hbar\omega = 2.4$ eV may be associated with electron transitions from the occupied $d(\downarrow)$ states lying just below the Fermi level into the empty $d(\downarrow)$ states above the Fermi level (near the peak of the density of electron states for fcc Co).[25]

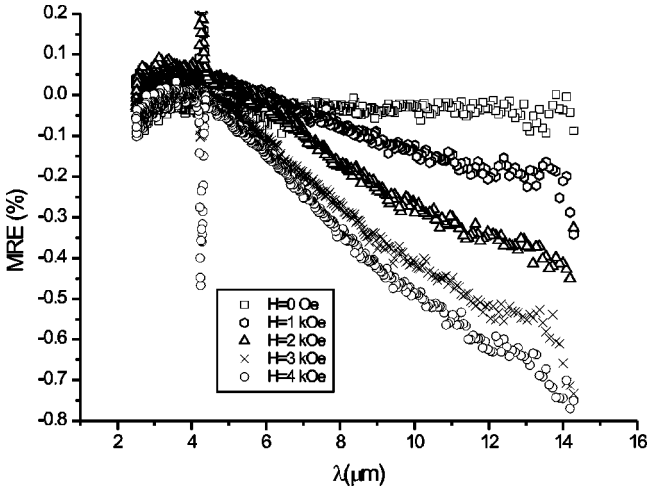

FIG. 6. Field dependence of the infrared reflection for $Co_{38}Ag_{62}$.

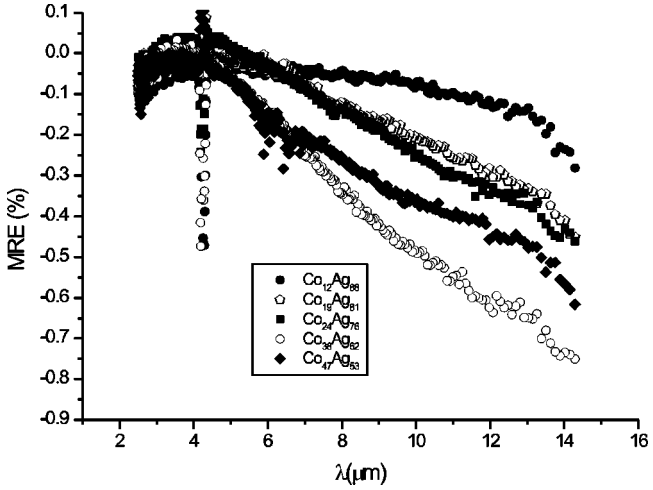

FIG. 7. MRE as a function of wavelength for different Co concentrations for $H = 4$ kOe.

Using a Drude expression, it is possible to estimate the dielectric functions $\varepsilon_1(\hbar\omega)$ and $\varepsilon_2(\hbar\omega)$ for Ag-rich granular films:

$$\varepsilon_1 = \varepsilon_r - \frac{\omega_p^2 \tau^2}{1+\omega^2\tau^2}, \tag{4}$$

$$\varepsilon_2 = \frac{\omega_p^2 \tau}{\omega(1+\omega^2\tau^2)}. \tag{5}$$

In Eqs. (4) and (5), $\hbar\omega_P$ is the ''quasifree'' plasma frequency of bulk Ag (9.1 eV) and $\hbar\tau^{-1}$ is the relaxation frequency of Ag (0.104 eV).[17,18] The real and imaginary parts of the dielectric function for Ag were first calculated using the Drude model $\varepsilon(\hbar\omega)$ with $\varepsilon_r = 1$ and are plotted in Figs. 2 and 4. From the poor agreement between the Drude model of $\varepsilon_1(\hbar\omega)$ and $\varepsilon_2(\hbar\omega)$ and the experimental data it can be concluded that the frequency dependence of the dielectric function of Ag-rich Co-Ag granular films is considerably different from the simple Drude model in which the scattering rate and plasma frequency are grain-size independent. The introduction of a value of $\varepsilon_r \approx 3.5$ improves the agreement between the Drude model predictions and observation for ε_1 but strong discrepancies remain for ε_2.

TABLE I. Comparative table of experimental values of GMR and predicted MRE as a function of the Co concentration (ρ in $\mu\Omega$ cm and $\lambda = 14\ \mu$m).

Co (at %)	$\rho\,(H=4$ kOe)	$\rho\,(H=0)$	$\mathrm{GMR}_{\mathrm{meas}}$ (%)	$\mathrm{MRE}_{\mathrm{calc}}$ (%)
10	23.30	24.25	4.0	−0.09
15	24.87	26.80	7.2	−0.17
20	26.75	29.50	9.3	−0.23
25	26.90	30.80	12.7	−0.32
30	28.40	31.88	10.8	−0.28
35	32.6	35.95	9.2	−0.25
40	40.30	43.10	6.5	−0.20

The grain size affects the scattering rate and can therefore be incorporated into the model by modifying τ in Eqs. (4) and (5). In these giant magnetoresistive materials, τ is also spin dependent. In Sec. IV B, the model of Zhang and Levy[2] is used to define these spin-dependent relaxation times [Eqs. (12)–(17)]. These values combined with $\varepsilon_r = 3.5$ were then used in Eqs. (4) and (5) to introduce grain-size effects into the model for ε_1 and ε_2 and the resulting curves are plotted in Figs. 2 and 4. This new model successfully describes the magnitude and general form of the dielectric tensor in this frequency regime, demonstrating the need to take into account the finite-size effects. The modified Drude model cannot, however, describe ε_2 in the region around the 2.4-eV absorption.

B. GMR and MRE

In the long-wavelength limit it is possible to interpret the MRE by a spin-dependent extension of the Hagen-Rubens relation.[17,18] In the absence of ferromagnetism the optical constants in the infrared take the form $n \approx k \approx (1/2\varepsilon_0\rho_0\omega)^{1/2}$, where ρ_0 is the low-frequency resistivity. Then at normal incidence the reflectivity R is given by

$$R \simeq 1 - [2\varepsilon_0\omega\rho_0]^{1/2}. \tag{6}$$

This is valid when $\omega\tau \ll 1$ for both electron spins, a condition typically satisfied for $\lambda \gtrsim 25\ \mu$m. R depends directly on ρ_0 with no explicit dependence on τ: it is then possible to estimate the change in reflectivity associated with a change in resistivity by differentiating R with respect to ρ_0, giving

$$\Delta R = -[2\varepsilon_0\omega\rho_0]^{1/2} \times \mathrm{GMR}, \tag{7}$$

where $\mathrm{GMR} = \Delta\rho/\rho_0$.

It can be seen from this formula that to a first approximation, the MRE is proportional to the GMR, but also depends on the zero-field resistivity ρ_0 and the frequency ω. Equation (7) can be used to calculate values for the MRE using the measured electrical resistivities. These values, calculated at $\lambda = 14\ \mu$m, are tabulated in Table I as a function of Co concentration along with measured resistivities and values of the GMR. The calculation predicts that the maximum MRE should occur when the GMR is at a maximum. In this study where the GMR is varied by changing the Co concentration, the theory predicts a maximum for the MRE at 25% Co, where the maximum GMR occurs. However, if the experimental values of the GMR and MRE as a function of Co concentration are compared, see Fig. 8, it is observed that the maxima for the GMR and MRE are obtained at different concentrations. In the case of the MRE, a maximum of −0.75% occurs at 38% Co, whereas the GMR reaches a maximum of −12.7% at 25% Co. The values in both cases are measured for $H = 4$ kOe. The trends in the data also indicate that the MRE is more significant for higher Co concentrations. These observations indicate that at $\lambda = 14\ \mu$m the conditions for the Hagen-Rubens relations are not met as $\omega\tau$ is approaching unity. As the wavelength is further reduced, optical parameters such as the plasma frequency and ε_r start to become significant. As the Co concentration is changed, microstructural changes occur that will affect these optical parameters.

Jacquet and Valet developed a multiparameter model for the analysis of the magnetorefractive effect and calculated expressions for the optical characteristics of a metal film, which are a function of the frequency-dependent conductivity in multilayer systems.[6] However, in their model, the ''quasifree'' plasma frequency is assumed to be a constant for all samples, which is inconsistent with observed optical properties of granular material systems as demonstrated in our study. For granular systems, ω_p and ε_r depend on concentration and microstructure, and to fit the dielectric properties with Eqs. (4) and (5), the parameter ω_p would need to have frequency dependence. Our theoretical analysis is based on the theoretical models developed by Granovsky, Kuzmichev, and Clerk[20] and van Driel *et al.*[8] This model avoids the need to include the frequency-dependent plasma frequency by using the relative dielectric constant ε_r to describe the optical behavior.

From the analysis of Eq. (6) and the experimental demonstration of the link between the GMR and the MRE, it is clear that the optical conductivity in the IR region is spin dependent. The complex refractive index is given by

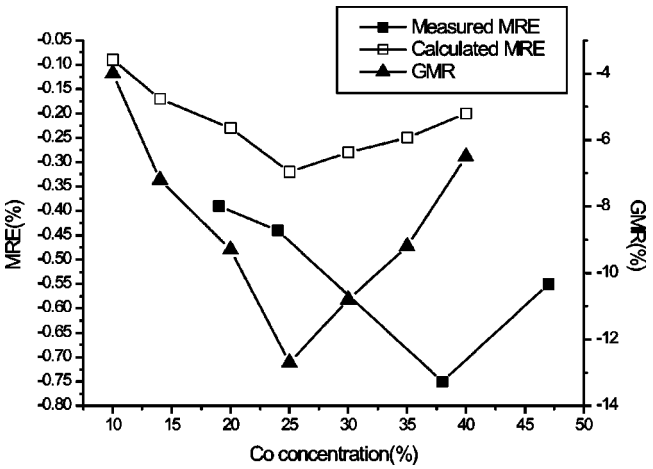

FIG. 8. Comparison of experimental GMR with both experimental and calculated MRE as a function of Co concentration for $H = 4$ kOe and $\lambda = 14\ \mu$m. The MRE is calculated with the preliminary model, which uses Eq. (7).

$$n-ik=\sqrt{\varepsilon_r-\frac{i\sigma(\omega)}{\varepsilon_0\omega}}, \tag{8}$$

with $\varepsilon_0=8.85\times10^{-12}$ A s/V m is the permittivity of free space, ε_r is the relative dielectric constant of metal, which depends on the contribution due to bound electrons, and $\sigma(\omega)$ is the conductivity. For metal films, ε_r typically varies between 1 and 10 and does not vary with frequency. In this study, *n* and *k* were determined from the ellipsometry experiments measured at $\lambda=1\ \mu$m and used to determine a value for ε_r for Ag-rich samples using Eq. (8). In this way the significant differences in optical properties between the samples were determined. In the MRE calculation, a value of $\varepsilon_r=3.5$ was used for all samples.

Having determined ε_r for each sample, Eq. (8) can then be applied in the IR region in order to calculate *n* and *k* and then the complex Fresnel reflection coefficient can be calculated for *s* and *p* polarization using

$$r^s=\frac{n_0\cos\phi_0-(n-ik)\cos\phi}{n_0\cos\phi_0+(n-ik)\cos\phi}, \tag{9}$$

$$r^p=\frac{(n-ik)\cos\phi_0-n_0\cos\phi}{(n-ik)\cos\phi_0+n_0\cos\phi}, \tag{10}$$

where ϕ_0 is the angle of incidence, which in this case was 75°, and $n_0=1$ for air.

In order to complete the calculation of the MRE using Eq. (8), a value for the optical conductivity $\sigma(\hbar\omega)$ must be calculated. In the infrared spectral region, the optical conductivity is the sum of contributions from spin-up (↑) and spin-down (↓) electrons:[7,8]

$$\sigma(\hbar\omega)=\sum_{\uparrow,\downarrow}\frac{\sigma^{\uparrow(\downarrow)}(\omega=0)}{1+i\omega\tau^{\uparrow(\downarrow)}}, \tag{11}$$

where $\sigma^{\uparrow}(\omega=0)$, $\sigma^{\downarrow}(\omega=0)$, and $\tau^{\uparrow}$ and $\tau^{\downarrow}$ are the spin-dependent dc conductivity and relaxation times, respectively. $\sigma^{\downarrow}(\omega=0)$, $\tau^{\uparrow}$, and $\tau^{\downarrow}$ must be determined from a model of the GMR in granular systems, which will enable the correlation between the GMR and MRE to be determined.

The magnitude of the GMR in granular films depends on the polarization of the magnetic material, the magnitude of the spin-dependent scattering, and the spin-diffusion length. The variation of resistance with applied field is proportional to $(M/M_s)^2$ provided there are no interparticle interactions.[26,27] We have used the model of Zhang and Levy[2,12] for GMR in granular systems to determine values of $\tau^{\uparrow}$ and $\tau^{\downarrow}$ needed for the MRE calculation. This model assumes that in granular systems the current is neither parallel nor perpendicular to the magnetic cluster surfaces and that it is valid to consider self-averaging of the scattering. They showed that spin-dependent scattering from the interfaces dominated over the bulk scattering from within the grains, generating a grain-size dependence of the GMR. In this model the GMR and spin-dependent conductivity can be written as

$$\mathrm{GMR}=\frac{\Delta\rho}{\rho(H=0)}=\frac{\xi_1^2}{\xi_0^2}\left(\frac{M}{M_s}\right)^2 \tag{12}$$

with

$$\xi_0=\frac{1-x}{\lambda_{n\dot{m}}}+\frac{x(1+p_b^2)}{\lambda_m}+\frac{3x(1+p_s^2)}{r_g\lambda_s/a_0}, \tag{13}$$

$$\xi_1=\frac{2xp_b}{\lambda_m}+\frac{6xp_s}{r_g\lambda_s/a_0}, \tag{14}$$

$$\sigma^{\uparrow(\downarrow)}(\omega=0)=\frac{ne^2\hbar}{2m}\frac{1}{\Delta^{\uparrow(\downarrow)}}, \tag{15}$$

$$\Delta^{\uparrow(\downarrow)}=\frac{\hbar}{2\tau^{\uparrow(\downarrow)}}, \tag{16}$$

$$\Delta^{\uparrow(\downarrow)}=\frac{E_F}{k_F}\left(\xi_0\pm\xi_1\frac{M}{M_S}\right), \tag{17}$$

where *x* is the concentration of ferromagnetic material, a_0 the lattice constant of the magnetic clusters, r_g the size of the magnetic grains, λ_{nm} and λ_m the mean free paths for the nonmagnetic matrix and the magnetic particles, respectively, λ_s the mean free path at the interfaces, p_b the ratio of spin-dependent to independent scattering potentials within the magnetic clusters, and p_s are the interfaces.

The grain size and Co concentration are known from experiment; all other parameters were taken from the literature[2] and are listed in Table II. In this model, with these parameters, the value of the giant magnetoresistance is dominated by the value of p_s and so this parameter was used to fit our experimentally determined values of resistivity. The results can be seen in Table II. These values were then used to obtain values for $\sigma^{\uparrow(\downarrow)}(\omega=0)$, $\tau^{\uparrow}$ and $\tau^{\downarrow}$ as a function of Co concentration. These parameters in conjunction with experimental data were then used to calculate the optical conductivity using Eqs. (11)–(17).

Using Eqs. (9) and (10), the MRE was then calculated as a function of wavelength. At this stage it is useful to put the MRE computation of the Levy-Granovsky (LG) model[20] into an analytical contact. In the far infrared (ω small), the effect should reach the spin-dependent Hagen-Rubens limit of Eq. (7) with $\Delta R\propto\lambda^{-1/2}$. Expanding $\sigma(\hbar\omega)$ in powers of $\omega\tau_{\uparrow(\downarrow)}$, it is possible to estimate ΔR as a series in powers of λ in the form

$$\Delta R=-\alpha\lambda^{-1/2}+\beta\lambda^{-3/2}+O(\lambda^{5/2}). \tag{18}$$

Here α is consistent with the value derived from the alternative approach in Eq. (7), and β is typically 3–5α for the samples studied here. In Fig. 9, the MRE is compared for the Hagen-Rubens (HR) model ($\beta=0$), the extended HR formula with typical sample parameters [Eq. (18)], and the numerical computation for the dielectric model. Above $\lambda\sim25\ \mu$m, all the models agree since $\omega\tau_{\uparrow(\downarrow)}$ is much less than unity, but at lower λ, values of $\omega\tau_{\uparrow(\downarrow)}$ become significant. Instead of becoming larger in magnitude according to the HR

TABLE II. Values of the fitting parameters used for the calculation of the MRE for various concentrations of Co.

Parameters	$Co_{12}Ag_{88}$	$Co_{19}Ag_{81}$	$Co_{25}Ag_{75}$	$Co_{38}Ag_{62}$	$Co_{46}Ag_{54}$
Grain diameter (nm)	1.8	2	3	3.5	4
Co mean free path, λ_m (nm)	5	5	5	5	5
Ag mean free path, λ_{nm} (nm)	35	35	35	35	35
Interface mean free path, λ_s	1.0	1.0	1.0	1.0	1.0
Bulk contribution, p_b	0.2	0.2	0.2	0.2	0.2
Interface contribution, p_s	0.19	0.23	0.275	0.255	0.17
$\Delta^{\uparrow}$ (eV)	0.245	0.298	0.347	0.445	0.433
$\Delta^{\downarrow}$ (eV)	0.145	0.158	0.165	0.22	0.259
GMR (%)	6.6	9.5	12.5	11.5	6.5

model, the extended HR model leads to a reduction in magnitude in agreement with the computed LG model; the two approaches agree well in the range 15–25 μm. However, below this we reach a regime where $\omega\tau_{\uparrow(\downarrow)}\sim 1$ and the expansion of Eq. (18) is inadequate. The MRE (%) changes sign and as the wavelength decreases further, the *d*-electron response begins to have some effect [simulated by the finite ε_r value in Eq. (4)]. The effects of different sample parameters in the LG model are shown in Fig. 10 for the experimental geometry used here with the following conclusions:

(i) the MRE has a nonlinear dependence on the wavelength over a wide-wavelength range of (5 to 30 μm); (ii) the absolute magnitude of the MRE rises with increasing wavelength in the region 2–30 μm and subsequently decreases at higher wavelengths; (iii) the variation of $\Delta R/R$ (or the MRE) strongly depends on the absolute values of optical constants *n* and *k* at small wavelengths; and (iv) in agreement with Ref. 20, the wavelength at which the minimum value of the MRE occurs increases with decreasing GMR. Comparison with the experimentally measured MRE (Fig. 7) leads to the following observations: (i) the change in reflectivity for the $Co_{38}Ag_{62}$ granular film is a factor of 5 larger at the maximum point compared to the MRE in $Co_{12}Ag_{88}$ in both the calculation and the experiment. This difference reflects the much smaller value of the real part ε_1 of the dielectric function for Co-rich films compared to Ag-rich Co_xAg_{1-x} granular films (Figs. 1 and 2); and (ii) the different dependence of the MRE and GMR on Co concentration as observed experimentally is now correctly predicted by the theory.

According to the Drude-Zener theory, the density of conduction electrons can be determined as in Ref. 18:

$$N \simeq \frac{|\varepsilon_1| m^* \pi c^2}{e^2 \lambda^2}. \tag{19}$$

The rapid decline of $\Delta R/R$ for Ag-rich Co_xAg_{1-x} granular films compared to the GMR (Figs. 7 and 10) is consistent with the ε_1 dependence on the Co content, which is due to the rapid reduction of electronic occupancy below the Fermi level due to the substitution of Co atoms by Ag atoms.[23]

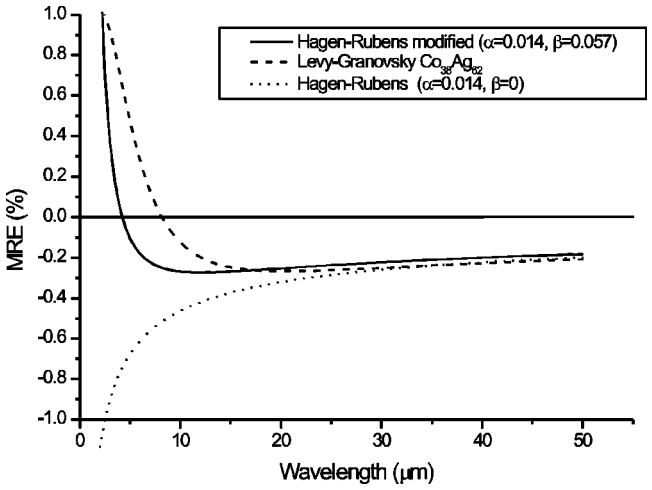

FIG. 9. Comparison of the different models for the MRE for normal incidence.

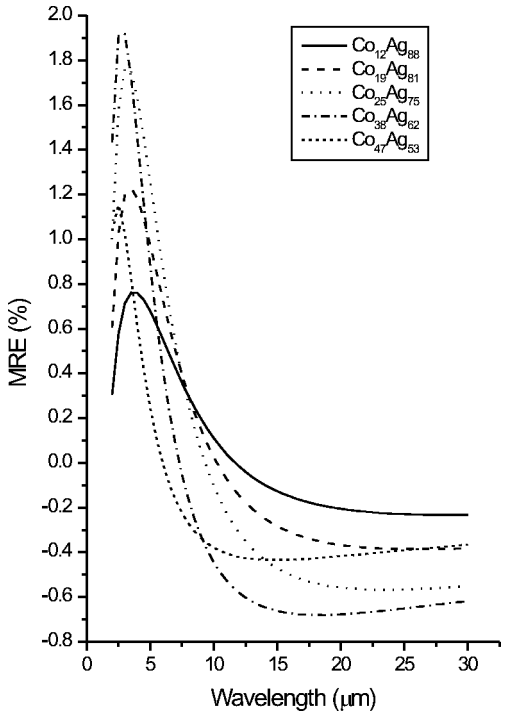

FIG. 10. Calculated values of the MRE (%) as a function of wavelength for different Co concentrations. The MRE is calculated with the extended LG model.

Below 5 μm the model predicts larger positive MRE values than is found experimentally: this is the region where a better description of *d*-electron response may be required.

V. CONCLUSIONS

A detailed analysis and comparison of the optical and electrical properties of Co_xAg_{1-x} giant magnetoresistive granular thin films has demonstrated the relationship between GMR and the MRE, leading the way for the MRE to be exploited as a contactless technique to measure the GMR. In the concentration range studied (x ranging from 0.07 to 0.7) the MRE increased with infrared wavelength in the range 4–14 μm. The shape of the MRE as a function of wavelength also changed as the GMR increased with a larger GMR and MRE, resulting in a more pronounced peak at low wavelengths.

Analysis of ellipsometry measurements showed that the plasma frequency and the optical relaxation rate are both functions of the composition and grain size, demonstrating that finite-size effects play an important role. The electrical and optical properties were shown to have a different dependence on the microstructure, therefore demonstrating that it is necessary to take this into account when calculating the MRE.

It was shown that for wavelengths greater than about 25 μm a modified Hagen-Rubens relation accurately describes the MRE and that in this region the GMR should be proportional to the MRE. As the wavelength is reduced, $\omega\tau$ becomes important, altering the shape of the MRE curve. At still lower wavelengths, the value of ε_r becomes significant. It is in these shorter-wavelength regimes that finite-size effects are most important.

A model for the MRE was developed based on the optical conductivity and the relative dielectric constant. Using the relative dielectric constant to describe the optical properties has the advantage that it is not frequency dependent and can be successfully determined experimentally from ellipsometry measurements in the visible optical spectral region. In this way the variation in optical properties as a function of Co concentration can be taken into consideration. This model successfully reproduced the variation of magnitude and shape of the MRE curve as a function of Co concentration and GMR.

As it is the spin-dependent relaxation time that appears in Eq. (8), the MRE is sensitive to this fundamental parameter rather than just the magnitude of the GMR as used in Eq. (7). The shape of the MRE curve as a function of wavelength is therefore sensitive to the spin-dependent scattering parameters that determine the GMR. The details of this variation will be the subject of a future publication and should allow accurate fitting of the shape of the MRE curve as a function of wavelength in order to determine the spin-dependent relaxation time.

The MRE depends on the response of quasifree electrons near the Fermi level. GMR has two basic origins—spin-dependent scattering of electrons around E_F and spin dependence in the density of states at E_F. The current MRE models emphasize spin dependence in relaxation time (i.e., in scattering). Although a close relationship between the MRE and GMR is to be expected GMR probes excitations within kT of E_F, while the MRE probes responses of electrons at energies greater than kT, typically in the order of 0.1 eV. While very close correspondence between the MRE and GMR is to be expected for low-energy (high wavelength $\gtrsim$25 μm) photons, more subtle relationships are to be expected at lower wavelengths as the results of this paper demonstrate.

ACKNOWLEDGMENTS

The financial support of the EPSRC and Seagate Technology is gratefully acknowledged.

[1] M. N. Baibich, J. M. Broto, A. Fert, F. Nguyen Van Dau, F. Petroff, P. Etienne, G. Creuset, A. Freiederich, and J. Chazellas, Phys. Rev. Lett. **61**, 2472 (1988).

[2] Shufeng Zhang and Peter M. Levy, J. Appl. Phys. **73**, 5315 (1993).

[3] E. Yu Tsymbal and D. G. Pettifor, Phys. Rev. B **54**, 15 314 (1996).

[4] A. Barthelemy, A. Fert, and F. Petroff, *Giant Magnetoresistance in Magnetic Multilayers*, Handbook of Magnetic Materials Vol. 12, edited by K. H. J. Buschow (Elsevier Science, North-Holland, Amsterdam, 1999).

[5] R. Coehoorn, M. A. M. Gijs, P. Grünberg, T. Rasing, K. Röll, and H. A. M. van den Berg, *Magnetic Multilayers and Giant Magnetoresistance: Fundamentals and Industrial Applications*, edited by Uwe Hartmann, Springer Series in Surfaces Science, Vol. 37 (Springer, New York, 2000).

[6] J. C. Jacquet and T. Valet, in *Magnetic Ultrathin Films, Multilayers and Surfaces*, edited by E. Marinero (Materials Research Society, Pittsburgh, 1995).

[7] S. Uran, M. Grimsditch, E. Fullerton, and S. D. Bader, Phys. Rev. B **57**, 2705 (1998).

[8] J. van Driel, F. R. de Boer, R. Coehoorn, and G. H. Rietjens, Phys. Rev. B **60**, 6949 (1999).

[9] M. Gester, A. Schlapka, R. A. Pickford, S. M. Thompson, J. P. Camplin, J. K. Eve, and E. M. McCash, J. Appl. Phys. **85**, 5045 (1999).

[10] John P. Camplin, Sarah M. Thompson, Ducan R. Loraine, David I. Pugh, Joanna Collingwood, Elaine M. McCash, and Andrew B. Horn, J. Appl. Phys. **87**, 4846 (2000).

[11] S. Honda, N. Nawate, M. Tanaka, and T. Okada, J. Appl. Phys. **82**, 764 (1997).

[12] F. Parent, J. Tuaillon, L. B. Stern, V. Dupuis, B. Prevel, A. Perez, P. Melinon, G. Guiraund, R. Morel, A. Barthelemy, and A. Fert, Phys. Rev. B **55**, 3683 (1997).

[13] M. B. Stearns and Y. Cheng, J. Appl. Phys. **75**, 6894 (1994).

[14] S. Y. Wang, W. M. Zheng, D. L. Qian, R. J. Zhang, Y. X. Zheng, Sh. M. Zhou, Y. M. Yang, B. Y. Li, and L. Y. Chen, J. Appl. Phys. **85**, 5121 (1999).

[15] V. G. Kravets, D. Bozec, and S. Thompson, in *Joint European Magnetic Symposia, Grenoble, France, 2001* [J. Magn. Magn. Mater. (to be published)].
[16] R. M. A. Azzam and N. M. Bashara, *Ellipsometry and Polarized Light* (North-Holland, Amsterdam, 1977).
[17] F. Abeles, *Optical Properties of Solids* (Elsevier, Amsterdam, 1972).
[18] A. V. Sokolov, *Optical Properties of Metals* (Blackie, Glasgow, 1967).
[19] V. G. Kravets, A. K. Petford-Long, and A. F. Kravetz, J. Appl. Phys. **87**, 1762 (2000).
[20] A. B. Granovsky, M. V. Kuzmichev, and G. P. Clerk, J. Theor. Phys. **89**, 955 (1999).
[21] Yu. G. Pogorelov, G. N. Kakazei, J. B. Sousa, A. F. Kravets, N. A. Lesnik, M. M. Perreira de Azevedo, M. Malinowska, and P. Panissod, Phys. Rev. B **60**, 12 200 (1999).
[22] N. W. Ashcroft and N. D. Mermin, *Solid State Physics* (Holt-Saunders, New York, 1976).
[23] *Non Linear Optics in Metals*, edited by K. H. Bennemann (Clarendon, Oxford, 1998).
[24] H. Raether, *Excitation of Plasmons and Interband Transitions By Electrons*, Tracts in Modern Physics Vol. 88 (Springer, Berlin, 1980).
[25] S. Ostanin and H. Ebert, Phys. Rev. B **58**, 11 577 (1998).
[26] J. Q. Xiao, J. S. Jiang, and C. L. Chien, Phys. Rev. B **46**, 9266 (1992).
[27] K. Ounadjela, S. M. Thompson, J. F. Gregg, A. Azizi, M. Gester, and J. P. Deville, Phys. Rev. B **54**, 12 252 (1996).